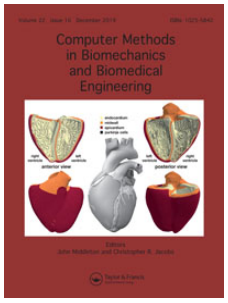

Taylor & Francis
Taylor & Francis Group

Computer Methods in Biomechanics and Biomedical Engineering

ISSN: 1025-5842 (Print) 1476-8259 (Online) Journal homepage: https://www.tandfonline.com/loi/gcmb20

Modeling and simulation of musculoskeletal system of human lower limb based on tensegrity structure

Zhanxi Wang, Chaoran Yang, Kang Feng & Xiansheng Qin

To cite this article: Zhanxi Wang, Chaoran Yang, Kang Feng & Xiansheng Qin (2019) Modeling and simulation of musculoskeletal system of human lower limb based on tensegrity structure, Computer Methods in Biomechanics and Biomedical Engineering, 22:16, 1282-1293, DOI: 10.1080/10255842.2019.1661389

To link to this article: https://doi.org/10.1080/10255842.2019.1661389

Published online: 05 Sep 2019.

COMPUTER METHODS IN BIOMECHANICS AND BIOMEDICAL ENGINEERING
2019, VOL. 22, NO. 16, 1282–1293
https://doi.org/10.1080/10255842.2019.1661389

Modeling and simulation of musculoskeletal system of human lower limb based on tensegrity structure

Zhanxi Wang, Chaoran Yang, Kang Feng and Xiansheng Qin

School of Mechanical Engineering, Northwestern Polytechnical University, Xi'an, China

ABSTRACT

In this paper, a mechanical model of the skeletal muscle of human lower limb system is established by using the Hill muscle model and kinetic equation of the movement of lower extremities according to the attachment positions of skeletal muscle. State vector and neural control are delineated by the direct configuration method. Changes of gait and skeletal muscle stress during walking process are analyzed with energy consumption as objective function. Results illustrate that simulation data are in good agreement with actual walking gait data. Feasibility and correctness of the designed model and control behavior of skeletal muscle tension structure are also verified.

ARTICLE HISTORY
Received 23 January 2019
Accepted 26 August 2019

KEYWORDS
Tensegrity structure; lower limb model; motion analysis; gait simulation

1. Introduction

The movement performance of human lower limbs is closely related to a special tensegrity structure formed by muscle-bone-tendon (Caluwaerts et al. 2013; Akhtaruzzaman et al. 2016b). The lower limb system is driven by the contraction of muscle attached to bone and joints, with bone acting as lever and joint acting as pivot (Ananthanarayanan et al. 2012; Akhtaruzzaman et al. 2016a; Rajagopal et al. 2016). Multi-muscle contraction and sequential activity can dynamically change the number of driving forces and provide time-varying optimal driving force. The stiffness and elasticity of mechanism can be adjusted by dynamically regulating the leg muscle tension to adapt mass distribution, and energy consumption of human lower limbs (Jacquelin et al. 2019). Therefore, a model of shape and structure of musculoskeletal tensegrity system with high energy efficiency, high strength, low weight, and compactness is an important reference prototype for improving the overall performance of bionic and robotic legs (Garcia et al. 2011; Seok et al. 2012). Establishing a universal model and efficient control method of human lower limb system is greatly significant for furthering research of human motion mechanisms in order to facilitate the design of lower limb rehabilitation medical equipment and control strategies for humanoid robots (Klein and Lewis 2012; Akhtaruzzaman et al. 2017; Hwang et al. 2018).

Since the 1970s, models of human lower limb gait have been studied and analyzed. Cappozzo established a method to obtain a mathematical description of the most significant variables concerning the kinematics and dynamics of human locomotion (Cappozzo et al. 1975). Pandy studied the motion of lower limb swing phase and bipedal support phase by using a five-rigid-body model (Pandy and Berme 1988). With the development of science and computer technology, more and more complex lower limb models and control strategies are proposed, and the research direction is more detailed. McLean developed a dedicated 3-D model to investigate potential loads that could lead to knee injuries during exercise (Mclean et al. 2003). Seth developed OpenSim system and built a model based on it to study muscle function during walking and running (Seth et al. 2011). Pizzolato presented a real-time model based on OpenSim solving inverse kinematics and dynamics of lower limb without simplifications at 2000 frame per seconds with less than 31.5 ms of delay (Pizzolato et al. 2017).

The research works of human lower limb model and musculoskeletal system are basically independent of each other and have not been well integrated. Research on human lower limb model is more inclined to analyze the law of human motion, which is more used in rehabilitation equipment, humanoid robots, and other fields. Research on the

CONTACT Zhanxi Wang zxwang@nwpu.edu.cn

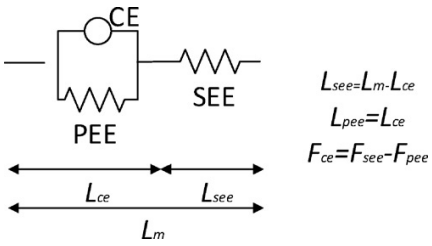

Figure 1. The three-element Hill muscle model.

musculoskeletal system is normally applied for physiological applications to study joint force, the specific information of muscle strength produced by human movement, and the accurate interpretation of neuromuscular coordination. Based on a bionic musculoskeletal model, this paper establishes the musculoskeletal movement model of human body and predicts human gait model under certain speed and gravity by optimizing function. This method involves musculoskeletal traction control and prediction of human gait under different gravity conditions in a human musculoskeletal model. It has certain reference significance for establishing a new control mode of humanoid robots, and it provides a train of thought on how to combine the human model with musculoskeletal system.

2. Methods

2.1. Skeletal muscle model

The Hill muscle model is used in analysis of muscle mechanics involved in this paper (Hill 1938). Assuming that there is a linear relationship between length of each muscle and joint angle, the relationship between muscle length and joint angle n ($n \leq 3$) is as follows:

$$L_m = a_0 + a_1\phi_1 + \cdots + a_n\phi_n \tag{1}$$

where L_m is the muscle length, ϕ_n is the angle of joint n, a_n is the length of the torque arm corresponding to joint n, and a_0 is the muscle length of model in the state of standing on both feet. The force produced by muscle is given by the three-element Hill model (as shown in Figure 1), and the muscle force model equation is derived by Van Soest, Bobbert, and Clean (van Soest and Bobbert 1993; Mclean et al. 2003; Jovanovic et al. 2015). The basic muscle force equation is

$$F_{\mathrm{CE}} = f(L_{\mathrm{CE}}) \cdot g(V_{CE}, a) \cdot \max\begin{Bmatrix} a_{\min} \\ a \end{Bmatrix} \tag{2}$$

$$F_{\mathrm{CE}} = F_{\mathrm{SEE}} - F_{\mathrm{PEE}} \tag{3}$$

$$F_m = F_{\mathrm{SEE}}(L_m - L_{\mathrm{CE}}) \tag{4}$$

where F_{CE} is the force on compression unit CE, F_{SEE} is the force on series elastic element SEE, L_{PEE} is the force on parallel elastic element PEE, L_{CE} is the length of CE, V_{CE} is the contraction speed of CE, a is the excitation of muscle, f is the mapping between force and length of CE, and g is the relationship mapping between force and excitation of CE, F_m is the ultimate force on muscle.

2.2. Dynamic model of human lower limbs

The model designed in this paper is a two-dimensional human lower limb system. Through mathematical methods, the kinematics and dynamics equations of two-dimensional model are established based on relationship of joint angles and Cartesian coordinate system of a key point. According to the characteristics of human lower limb movement, kinematics and dynamics simulation analysis of human lower limb system is further carried out.

The lower limb model is simplified as a seven-link mechanism, and the generalized coordinate system of lower limb model is established by using nine coordinates (X, Y, q_1, $q_2 \ldots q_7$). The method and process to establish generalized coordinate system are given in the Appendix.

Based on kinematics modeling, the relationship between each bone and joint torque in process of lower limb movement is studied. The Lagrange equation is used to establish system dynamics equation of a particle:

$$F_i = \frac{d}{dt}\frac{\partial L}{\partial \dot{q}_i} - \frac{\partial L}{\partial q_i}(i = 1, 2, \ldots n) \tag{5}$$

where q_i represents the generalized coordinates of joint i, $\dot{q}_i$ is the corresponding velocity, F_i is the nonconservative force acting on the joint i, and n is the number of links.

The kinetic energy of a rigid body can be expressed as sum of the translational kinetic energy of center of mass and rotational kinetic energy around center of mass. It is a function of generalized coordinate q and generalized velocity $\dot{q}$, which is written as $K(q, \dot{q})$. The potential energy of a rigid body is a function of the generalized coordinate q, which is written as $V(q)$. Lagrange's equation can be deduced as

$$\frac{d}{dt}\frac{\partial K(q,\dot{q})}{\partial \dot{q}_i} - \frac{\partial K(q,\dot{q})}{\partial q_i} + \frac{\partial V(q)}{\partial q_i} = F_i \tag{6}$$

Assuming that Cartesian coordinates of the center of mass of link i are (p_i^x, p_i^y), it can be expressed as a function of generalized coordinates q:

$$\begin{bmatrix} p_i^x \\ p_i^y \end{bmatrix} = \begin{bmatrix} p_i^x(q) \\ p_i^y(q) \end{bmatrix} \tag{7}$$

The linear velocity and absolute angular velocity of link i can be obtained by derivation of Eq. 7:

$$\begin{bmatrix} \dot{p}_i^x \\ \dot{p}_i^y \end{bmatrix} = \begin{bmatrix} \frac{\partial p_i^x(q)}{\partial q} \\ \frac{\partial p_i^y(q)}{\partial q} \end{bmatrix} \dot{q} \tag{8}$$

The kinetic energy of link i can be written as

$$\begin{aligned} K_i &= \frac{1}{2} m_i \left((\dot{p}_i^x)^2 + (\dot{p}_i^y)^2 \right) + \frac{1}{2} J_i (\dot{q}_i)^2 \\ &= \frac{1}{2} \dot{q}^T D_i(q) \dot{q} \end{aligned} \tag{9}$$

where $D_i(q) = m_i \left((\frac{\partial p_i^x}{\partial q})^2 + (\frac{\partial p_i^y}{\partial q})^2 \right) + J_i$ is the inertia matrix.

The total kinetic energy of system is

$$K = \sum_1^n K_i = \frac{1}{2} \dot{q}^T D(q) \dot{q} \tag{10}$$

The potential energy of link i is

$$V_i = m_i g p_i^y \tag{11}$$

The total potential energy of system is

$$V = \sum_i^n V_i = \sum_i^n m_i g p_i^y \tag{12}$$

The first item on Left Hand Side of Eq. 6 can be obtained as

$$\begin{aligned} \frac{d}{dt} \frac{\partial K(q, \dot{q})}{\partial \dot{q}_i} &= \frac{d}{dt} \left(\sum_{j=1}^n D_{ij}(q) \dot{q}_i \right) \\ &= \sum_{j=1}^n D_{ij}(q) \ddot{q}_i + \sum_{j,k=1}^n \frac{\partial D_{ij}(q)}{\partial q_k} \dot{q}_j \dot{q}_k \end{aligned} \tag{13}$$

The second item on Left-Hand Side of Eq. 6 can be expanded:

$$\frac{\partial K(q, \dot{q})}{\partial q_i} = \frac{1}{2} \sum_{j,k=1}^n \frac{\partial D_{kj}(q)}{\partial q_i} \dot{q}_j \dot{q}_k \tag{14}$$

Then Eq. 6 can be expressed as

$$\begin{aligned} &\sum_{j=1}^n D_{ij}(q) \ddot{q}_i + \sum_{j,k=1}^n \left(\frac{\partial D_{ij}(q)}{\partial q_k} \dot{q}_j - \frac{1}{2} \frac{\partial D_{kj}(q)}{\partial q_i} \dot{q}_j \right) \dot{q}_k \\ &\quad + \frac{\partial V(q)}{\partial q_i} = F_i \end{aligned} \tag{15}$$

The Right-Hand Side of Eq. 14 can be written as a vector form Γ_{ijk}:

$$\Gamma_{ijk} = \frac{1}{2} \left(\frac{\partial D_{ij}(q)}{\partial q_k} + \frac{\partial D_{ik}(q)}{\partial q_j} - \frac{\partial D_{kj}(q)}{\partial q_i} \right) \tag{16}$$

The dynamic equation can be written as

$$D(q) \cdot \ddot{q} + C(q, \dot{q}) \cdot \dot{q} + G(q) = F \tag{17}$$

where $C_{ij}(q, \dot{q}) = \sum_{k=1}^n \Gamma_{ijk}(q) \dot{q}_k$, and $G_i(q) = \frac{\partial V(q)}{\partial q_i}$.

The non-conservative force can be decomposed into $F_i = u_i + E'(q) \cdot F_{\text{ext}}$, where u_i is the driving torque acting on joint i, F_{ext} is the other non-conservative force except the joint driving torque, and $E_i(q)$ is Jacobian matrix of Cartesian coordinates for the generalized coordinates of the external force F_{ext} acting point. According to the specific form of lower limb system, the joint torque u is equal to zero, and the driving force is a non-conservative force provided by skeletal muscle models. Assuming that the attachment points of a muscle are i and j, its Cartesian coordinates are (x_i, y_i) and (x_j, y_j) in the absolute coordinate system. By expressing Cartesian coordinates as an equation of the generalized coordinate q, Jacobian matrix of Cartesian coordinates for generalized coordinates of the external force acting point can be determined:

$$\begin{bmatrix} x_i \\ y_i \end{bmatrix} = \begin{bmatrix} x_i(q) \\ y_i(q) \end{bmatrix} = E_i(q) q. \tag{18}$$

By assuming that a link i is subjected to K muscular forces, which is expressed as F_{cen} $(n = 1,2, \ldots k)$, the resultant force F_i is

$$F_i = \sum_{n=1}^k E'_i(q)_n F_{\text{cen}} \tag{19}$$

Muscular forces are related to muscle length L_m and compression unit l_{ce} in the Hill muscle model, and L_m can be expressed as

$$L_m = \sqrt{(x_i - x_j)^2 + (y_i - y_j)^2} = L_m(q) \tag{20}$$

Then, Eq. 19 can be written as

$$F_i = \sum_{n=1}^k E'_i(q)_n \cdot F_{\text{cen}} \left(L_m(q), l_{\text{ce}} \right) \tag{21}$$

The final kinetic equation of model can be written as a second-order differential equation:

$$D(q) \cdot \ddot{q} + C(q, \dot{q}) \cdot \dot{q} + G(q) = B \cdot u + E'(q) \cdot F_{\text{ext}} \tag{22}$$

where D is the inertia matrix, C is the Coriolis matrix, G is the gravity moment vector, B is the input matrix,

Table 1. Parameters of the human lower limb system model.

Section	Length (mm)	Weight (kg)
Trunk	Chest width: 305, chest thickness: 233, buttock width: 327, height: 635	29.82
Thighs	Length: 495, sitting thigh thickness: 233	9.8
Calves	Length: 397	2.8
Foot	Length: 261, Width: 101, Height: 76	1.05

u is the driving moment matrix, F_{ext} is the other non-conservative force except the joint driving torque, and E is the Jacobian matrix of Cartesian coordinates for generalized coordinates of the external force acting point.

2.3. Direct collocation method

The direct collocation method is widely used to solve nonlinear trajectory optimization problems (Betts 1998; Kaplan and Heegaard 2001; Ackermann and van den Bogert 2010; Ackermann and van den Bogert 2012). The direct collocation method can transform the dynamic equation constraints of system into equality constraints on state vectors by discretization and then construct nonlinear programming problem.

By defining the objective function of system optimization as J, the dynamic equation of system can be written as

$$\frac{d\chi}{dt} = F(\chi), t \in [T_0, T_1] \tag{23}$$

where χ is the state variable. The time interval $[T_0, T_1]$ will be divided into N time intervals of equal length; the first time node is t_0, and the last time node is t_n. The dynamic equation can be approximated by interpolation in the time interval of two adjacent time nodes. At time node t_k, the state vector equation can be written as follows:

$$\frac{\chi_k - \chi_{k-1}}{t_k - t_{k-1}} = \dot{\chi}_k \tag{24}$$

Then, the direct collocation method transforms control problem into finding optimal trajectory sequence$(\chi_0, \chi_1, \ldots, \chi_N)$ and duration $(t_0, t_1, \ldots, t_N)$ with discretization. The discrete form of objective function J is minimized, which satisfies the existence of corresponding dynamic equation constraints and corresponding boundary conditions constraints at each time node.

In this way, an infinite-dimensional optimal control problem is transformed into a finite-dimensional nonlinear programming problem by the direct collocation method.

3. Modeling and simulation

3.1. Modeling of the human lower limb system

The human lower limb system designed in this paper is composed of seven parts (including trunk, two thighs, two calves, and two feet), which are confined in a sagittal plane. The system has six degrees of freedom (Hardin et al. 2004). Park's relevant research (Park 2008) shows that arm swing in sagittal plane will only have a slight impact on human gait, so the two-dimensional lower limb system is suitable for studying human gait characteristics and muscle tension control system simulation. In this paper, the human lower limb system is modeled in MATLAB. The human body data used in modeling process are Chinese adult human body size data provided by GB-10000-88. The specific parameters of model are shown in Table 1, which are average values of 26–35 years old adult males with height of 1775 mm and weight of 70 kg.

Based on analysis of human muscle mechanics, eight related muscles with the most obvious effects on movement of human lower limbs were identified as the source of force input to lower limb model. They are psoas (PSOAS), gluteus (GLU), hamstring (HAM), rectus femoris (RF), vasti (VAS), gastrocnemius (GAS), soleus (SOL), and tibialis-anterior (TA). According to human anatomy data (Gerritsen et al. 1998), the locations of muscle attachment points are determined. The relevant parameters of eight selected muscles are shown in Table 2.

The model of human lower limb system with eight muscle actuators is shown in Figure 2.

3.2. Gait simulation of the human lower limb model

According to the Hill muscle model and lower limb model, the state vector of skeletal muscle model is established as $\chi = [\, q^T \quad \dot{q}^T \quad l_{ce}^T \quad a^T \,]^T$. The state vector includes 50 variables, where vector q includes 9 generalized coordinates, vector $\dot{q}$ includes 9 generalized velocities, vector L_{CE} includes 16 muscle compression unit lengths, and vector a includes 16 muscle stimulation values. The relationship between these variable groups can be expressed as four equations:

Table 2. Main parameters of selected muscles.

Muscle (group)	F_{max} (N)	L_{Ceopt} (m)	Width (%L_{CEopt})	L_{slack} (m)	a_0 (m)	a_{ankle} (m)	a_{knee} (m)	a_{hip} (m)
PSOAS	821	0.102	129.8	0.142	0.248	0	0	−0.050
GLU	1705	0.200	62.5	0.157	0.271	0	0	0.062
HAM	1770	0.104	119.7	0.334	0.383	0	−0.034	0.072
RF	663	0.081	144.3	0.398	0.474	0	0.050	−0.034
VAS	7403	0.093	62.7	0.223	0.271	0	0.042	0
GAS	1639	0.055	88.8	0.420	0.404	0.053	−0.020	0
SOL	3883	0.055	103.9	0.245	0.201	0.053	0	0
TA	1528	0.082	44.2	0.317	0.464	−0.037	0	0

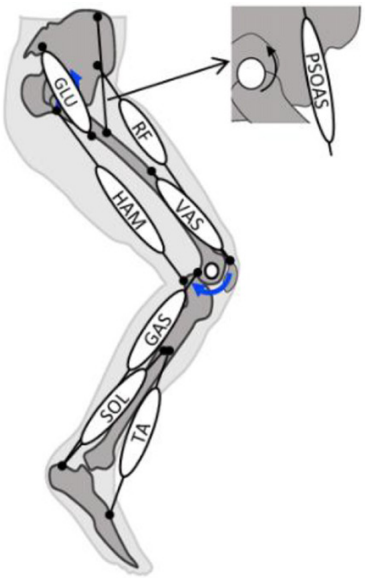

Figure 2. Human lower limb system model.

$$\dot{q} = I_{f\times f} \cdot \dot{q} \tag{25}$$

$$\ddot{q} = \ddot{q}(q, \dot{q}, l_{ce}) \tag{26}$$

$$\dot{l}_{ce} = \dot{l}_{ce}(q, l_{ce}, a) \tag{27}$$

$$\dot{a} = \dot{a}(a, u) \tag{28}$$

where $I_{f\times f}$ is the unit matrix. Equation 26 is derived from the lower limb system dynamics equation. Equation 27 is the velocity equation of a muscle contraction unit. Equation 28 is the functional relationship between muscle stimulation and nerve stimulation.

The contact force model between the foot and ground for human lower limb system model is composed of 10 uniformly distributed spring damping systems on the sole of the foot. The mathematical model of contact force in vertical direction of a single spring damping unit j can be expressed as follows (Clercq 1993):

$$f_{y,j} = a\delta_j^3(1 - b\dot{\delta}_j) \tag{29}$$

where δ_j is the contact depth between spring damping unit j and ground, a is the vertical stiffness parameter of damping spring j ($a = 5.0 \times 10^7 N/m^3$), and b is the vertical damping parameter of damping spring j ($b = 1.0s/m$).

The horizontal direction Coulomb force affected by contact element can be written as (van den Bogert et al. 1989)

$$f_{x,j} = \frac{1-e^{-v_{s,j}/v_c}}{1+e^{-v_{s,j}/v_c}}\mu f_{y,j} \tag{30}$$

where $v_{s,j}$ is the relative slip velocity of spring damping unit j, v_c is the scale factor ($v_c = 0.05m/s$), and the friction coefficient is $\mu = 1$.

The gait prediction problem of neuromuscular control can be expressed as finding the relationship curve $u(t)$ and state vector $\chi(t)$ between nerve excitation and time based on a given pace v. The gait characteristics, such as speed, step length, and rhythm, are closely related to the energy consumed in each step of the walking process. Thus, the energy consumption function is taken as the objective function. The problem becomes to solve the global minimum that satisfies the objective function of energy consumption in a gait cycle under the constraints of system dynamics.

The kinetic constraint is as follows:

$$\dot{\chi}(t) = f\Big(\chi(t), u(t), t\Big) \tag{31}$$

The boundary conditions are as follows:

$$0 \le u(t) \le 1 \tag{32}$$

The periodic expression is

$$\chi(T) = \chi(0) + vT\hat{\chi} \tag{33}$$

$$u(T) = u(0) \tag{34}$$

The energy consumption function is (Glitsch and Baumann 1997; Thelen and Anderson 2006)

$$J = \frac{1}{\sum V_i}\sum_{i=1}^{16}\frac{V_i}{T}\int_0^T a_i^2(t)dt \tag{35}$$

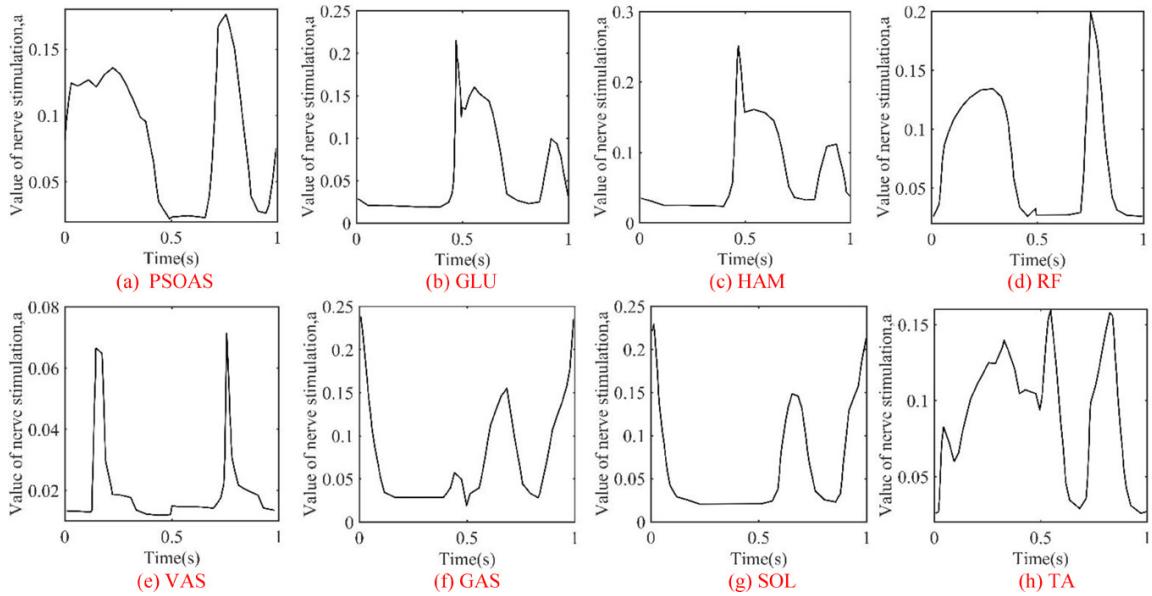

Figure 3. The variations of nerve excitation.

In the above equations, T is the gait cycle, $\hat{\chi}$ is the state space unit vector, and V_i is the muscle volume. The energy consumption function can complete calculation of energy by weighting stimulation of a single muscle affected by muscle volume.

The state vector and neural control can be discretized by direct collocation method, and the optimal value problem of neuromuscular control is transformed into a nonlinear programming problem. Based on hypothesis of bilateral symmetry, the human gait is considered to be symmetrical. In this paper, the gait period is divided into 100 equal time interval sequences. At time node t_k, the unknown variables are neural excitation variables $u(t_k)$, state vector $\chi(t_k)$, and period T. The state vector equation of system is same as Eq. 24.

The system dynamics constraint calculated by this method is a large-scale sparse matrix. In this paper, SNOPT toolbox is used to solve the nonlinear programming problem of large-scale sparse matrix in MATLAB.

3.3. Gait simulation and result analysis

Based on above data of human lower limb model and gait prediction method, the time-varying value of nerve excitation under a low gravity environment and walking speed of 1.1 m/s is obtained. The partial results are shown in Figure 3.

Figure 3 illustrates variations of nerve stimulation of eight muscles in the right leg during walking for a gait cycle. horizontal ordinate represents time, which is a complete gait cycle of 1 s, and longitudinal coordinate represents the value of nerve stimulation of muscles associated with human motion, which is a dimensionless value and satisfies $a \leq 1$. The value of nerve stimulation indicates output force and energy supply of muscle during exercise. The higher value of a, the more energy and greater output force it provides. According to time-varying curve of nerve stimulation, when walking in a low gravity environment, the value of nerve stimulation is less than 0.3, which indicates that the energy and force provided by muscle for human movement are smaller, and this gait is a kind of walking action that saves more strength. At the same time, if a value of one of the eight muscles is higher, it indicates that this muscle plays a greater role in human motion at this time. Observing the eight curves, it can be found that a value of vasti muscle group (VAS) is the lowest among all eight muscles (a value is no more than 0.1). The vasti muscle group (VAS) is responsible for knee joint stretching. However, in the whole gait movement process, knee joint will naturally produce stretching behavior affected by gravity. The vasti muscle group (VAS) plays a more auxiliary role and does not provide great force to drive knee joint stretching, so its nerve stimulation is the lowest of eight muscles.

According to the predicted results of nerve stimulation and the state vector values χ at each time node, the Hill muscle model is used to calculate real-time muscle force in MATLAB, and then it is applied to the model to realize muscle tensegrity effect. The human skeletal muscle's motion control is simulated in the process of movement, and the motion control of tensegrity structure is tested by simulating human skeletal muscle's actuation control and gait movement process. The process diagram of control system is shown in Figure 4. The human lower limb model control and simulation system is established in MATLAB. The calculation of muscle elongation and input can also be integrated in a same control module. Take psoas muscle as an example, its control module composition is shown in Figure 5.

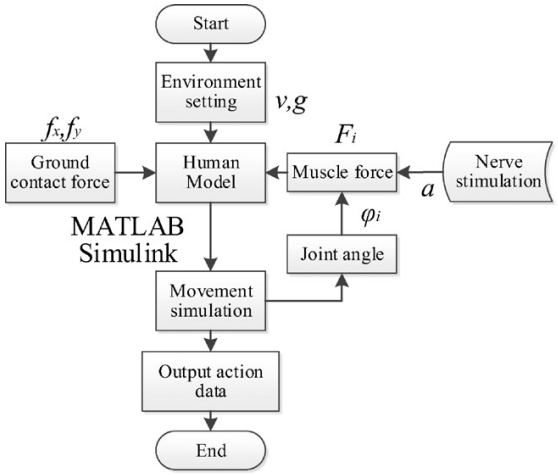

Figure 4. Process diagram of the control system.

Figure 5 is a custom Matlab Function control module for PSOAS muscles. Its purpose is to calculate muscle strength of PSOAS muscles at a certain time and output initial muscle length and contraction speed of next moment. The calculation is based on angle of hip, knee and ankle joint at current moment, the length and contraction speed of damping element in Hill model. In Figure 5, Module hip records angle of the current hip joint, Module knee records angle ofcurrent knee joint, Module ankle records angle of current ankle joint, and Module Clock is the timing module. The recorded values of above four modules are used as input part of MATLAB Function control module. The output part of control module has three items, which are muscle force at this moment, and the muscle length and contraction speed at next moment. The muscle force module can act on Prismatic module throughJoint Actuator module, which is a sliding pair on both sides of muscle PSOAS. The other two outputs are initial muscle length and contraction length at next moment, and two delayed modules are used transfer this two outputs as the feedback input of control module. Revolute module represents the connecting rotating pair of PSOAS muscle and trunk attachment point, and Revolute 1 module represents connecting rotating

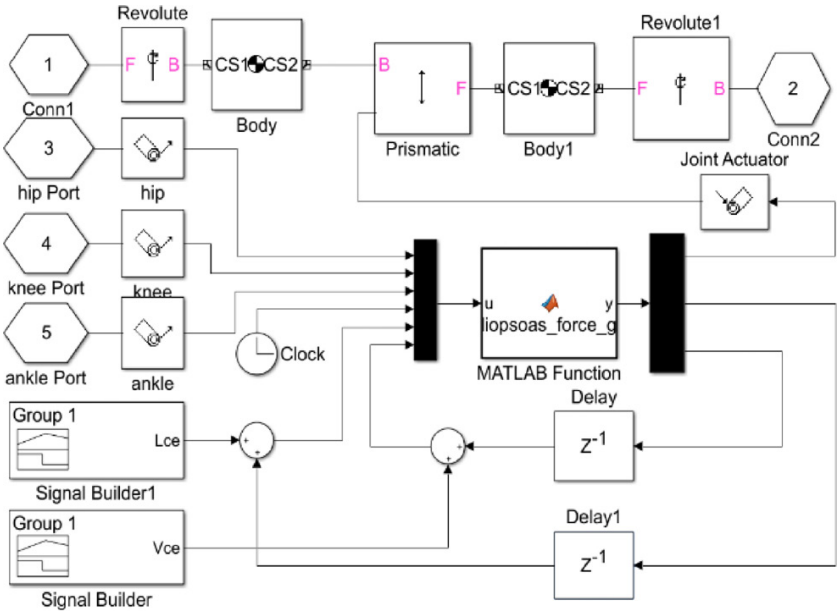

Figure 5. Control module diagram of muscle Psoas force.

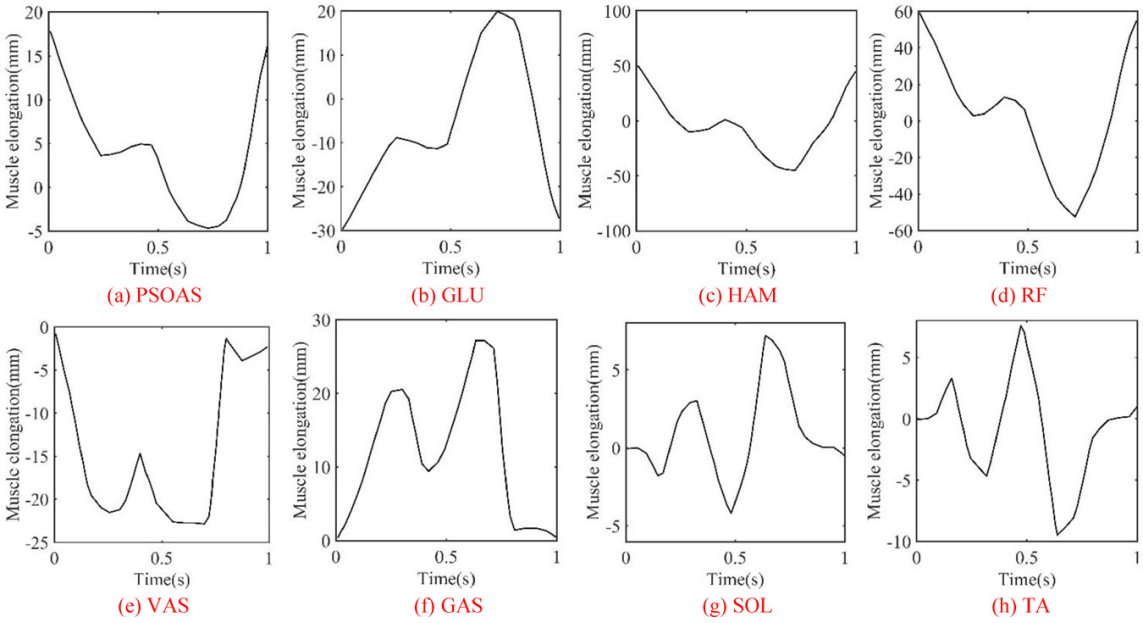

Figure 6. The variations of muscle elongation.

pair of PSOAS muscle and thigh attachment point. The Singal Builders in left corner are signal generator of length and contraction speed of damping element in Hill model.

The full closed-loop feedback control of tensegrity structure is realized by sensor module and function calculation module. During simulation, Figure 6 shows the variations of eight human muscles' elongations as a function of time during a gait cycle.

In Figure 6, horizontal ordinate represents time, which is a complete gait cycle of 1 s. Longitudinal coordinate represents muscle elongation. Zero point of longitudinal coordinate is the relative muscle length in natural standing state of human body. When muscle elongation is positive, it indicates that the muscle is stretched, and when muscle elongation is negative, it indicates that the muscle is contracted. It can be seen that the elongation changes of all eight muscles are less than 60 mm, which is consistent with the data of human anatomy and does not exceed the normal range of human muscle elongation. The elongation curves of eight muscles reflects corresponding joint movement trend to a certain extent. For example, Vasti muscle group (VAS) mainly drives extension of knee joint. During a whole gait cycle, the muscle elongation is negative, which means that the Vasti muscle group (VAS) has been in a contraction change. The reason is that knee joint always has a certain degree of bending during gait walking in a low gravity environment.

In a gait cycle ($t = 1$ s) of low gravity enviroment, the angle variations of the human joints obtained from the simulation process are compared with the joint angle curves in Ref. (Ackermann and van den Bogert 2012) as shown in Figures 7–9.

In Figure 7, it is illustrated that the joint angle of left hip reaches a minimum of −17° at 180 ms, and reaches a maximum of 31° at 495 ms in the simulation process. The joint angle of right hip decreases gradually in gait cycle, and reaches a minimum of −14° at 765 ms. Then it increases to 35° within the remaining 235 ms. In Figure 8, The angles of left knee joint and right knee joint are both negative. When supporting foot and opposite foot landing and leaving ground, wave crest and trough will be formed accordingly. In Figure 9, left ankle as contralateral foot ranges from −10° to 6°, and right ankle as supporting foot ranges from −12° to 8°.Through comparison of Figures 7–9, it can be found that overall trend of simulation results and Ref. (Ackermann and van den Bogert 2012) results are basically consistent. However, in simulation results, there are always several sudden changes in angle curve of each joint, which makes overall curves of joint angle more inclined to a broken lin. It is different from smooth change of joint angle in actual walking process. The reason may be

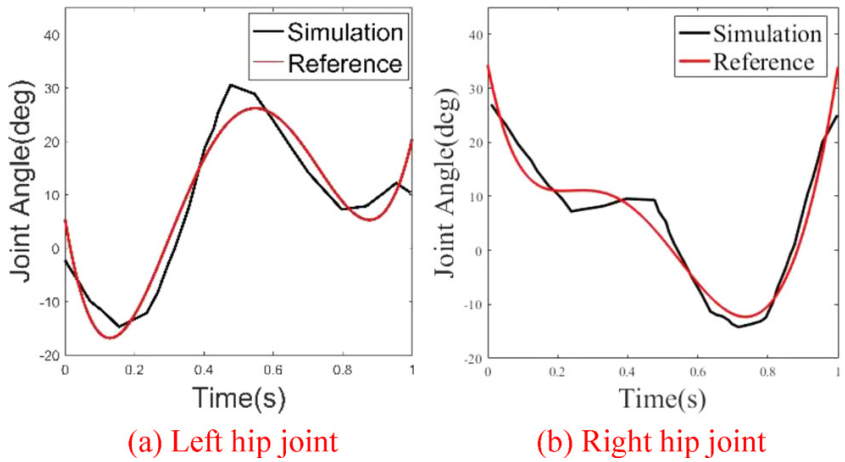

Figure 7. Hip angle variations in simulation.

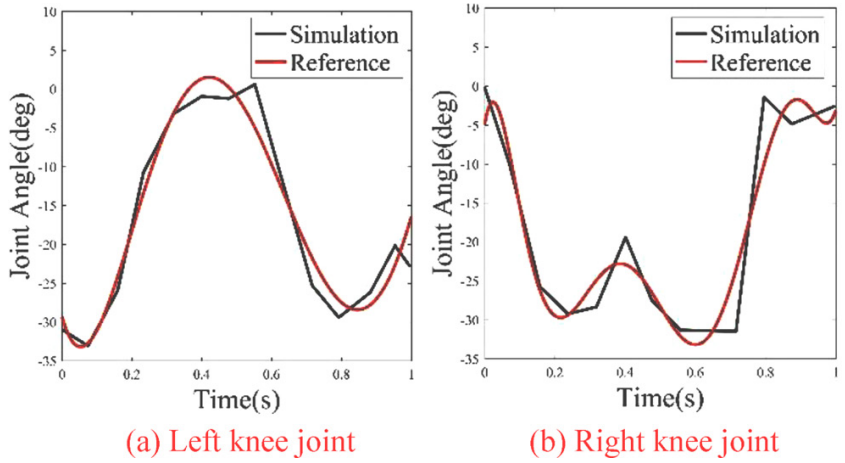

Figure 8. Knee angle variations in simulation a.

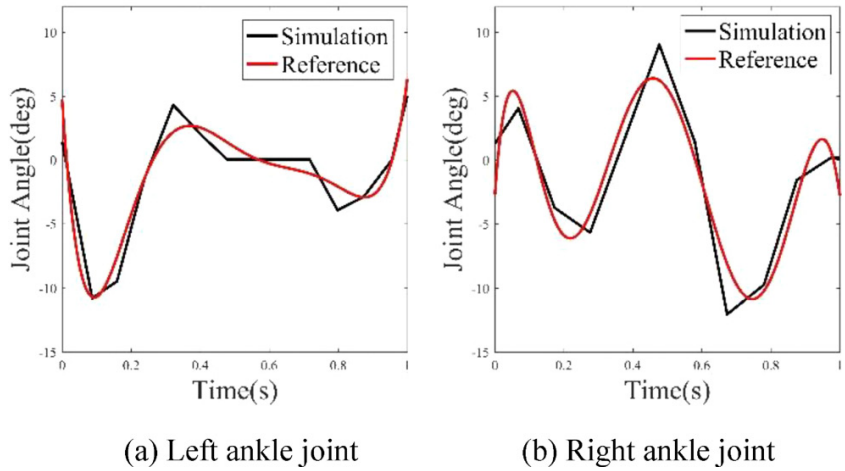

Figure 9. Ankle angle variations in simulation.

that only eight muscles related to exercise are selected in simulation model.

This result confirms the validity of human lower limb model and gait prediction method established in this paper, as well as validity of the driving mode of bionic tensegrity structure. It can be used for prediction of lunar walking gait and other research on gait research, bionic structure, humanoid robots and other fields.

4. Conclusion

The lower limb system of human skeletal muscle based on tensegrity structure is proved to be a compatible modeling method. Its gait prediction theory and tensegrity control method provide a new technical approach for research on bionics, humanoid robots, and other related fields and offer new ideas for the study and application of human models and skeletal muscle system. The tensegrity structure and gait prediction method designed in this paper are still complex and difficult to control. Firstly, according to the direct collocation method, state vector and contact model are reasonably constructed, and energy consumption is taken as optimization objective function. Then state vector at each time is calculated to predict human walking gait in a low gravity environment. In simulation process, the nerve stimulation and elongation of the eight muscles that drive the lower limb model movement need to be controlled simultaneously. This paper focuses more on kinematic simulation of human low limb. In the process of muscle driving, only changes of nerve stimulation and muscle elongation with time are considered. The next research will focus on dynamic analysis of related active muscles by combined force control methods and bionic muscle tensegrity structure.

Disclosure statement

No potential conflict of interest was reported by the authors.

Funding

This work is partially supported by the National Natural Science Foundation of China (Grant no. 51505380), Shaanxi Science and Technology Innovation Project (Grant no. 2016KTZDGY4-12), Henan Science Research and Development Special Project (Grant no. 182102210084), and the '111 project' of China (Grant no. B13044).

ORCID

Zhanxi Wang http://orcid.org/0000-0003-4650-7723

References

Ackermann M, van den Bogert AJ. 2010. Optimality principles for model-based prediction of human gait. J Biomech. 43(6):1055–1060.

Ackermann M, van den Bogert AJ. 2012. Predictive simulation of gait at low gravity reveals skipping as the preferred locomotion strategy. J Biomech. 45(7):1293.

Akhtaruzzaman M, Shafie A, Khan M. 2016. A review on lower appendicular musculoskeletal system of human body. IIUMEJ. 17(1):83–102.

Akhtaruzzaman M, Shafie AA, Khan MR. 2016. Gait analysis: Systems, technologies, and importance. J Mech Med Biol. 16(07):1630003.

Akhtaruzzaman M, Shafie AA, Khan MR. 2017. Quasi-inverse pendulum model of 12 DoF bipedal walking. Int J Autom Comput. 14(2):179–190.

Ananthanarayanan A, Azadi M, Kim S. 2012. Towards a bio-inspired leg design for high-speed running. Bioinspir Biomim. 7(4):046005.

Betts JT. 1998. Survey of Numerical Methods for Trajectory Optimization. J Guid Contr Dynam. 21:193–207.

Caluwaerts K, D'Haene M, Verstraeten D, Schrauwen B. 2013. Locomotion without a brain: physical reservoir computing in tensegrity structures. Artif Life. 19(1): 35–66.

Cappozzo A, Leo T, Pedotti A. 1975. A general computing method for the analysis of human locomotion. J Biomech. 8(5):307–320.

Clercq DD. 1993. Deformation characteristics of the heel region of the shod foot during a simulated heel strike: The effect of varying midsole hardness. J Sports Sci. 11: 449.

Garcia E, Arevalo JC, Muñoz G, Gonzalez-De-Santos P. 2011. On the biomimetic design of agile-robot legs. Sensors (Basel). 11(12):11305–11334.

Gerritsen KGM, van den Bogert AJ, Hulliger M, Zernicke RF. 1998. Intrinsic muscle properties facilitate locomotor control - a computer simulation study. Motor Control. 2(3):206–220.

Glitsch U, Baumann W. 1997. The three-dimensional determination of internal loads in the lower extremity. J Biomech. 30(11–12):1123–1131.

Hardin EC, Su A, van den Bogert AJ. 2004. Foot and ankle forces during an automobile collision: the influence of muscles. J Biomech. 37(5):637–644.

Hill AV. 1938. The heat of shortening and the dynamic constants of muscle. Proc Roy Soc Lond. 126:136–195.

Hwang B, Oh BM, Jeon D. 2018. An optimal method of training the specific lower limb muscle group using an exoskeletal robot. IEEE Trans Neural Syst Rehabil Eng. 26:830–838.

Jacquelin E, Brizard D, Dumas R. 2019. A screening method to analyse the sensitivity of a lower limb multibody kinematic model. Comput Methods Biomech Biomed Eng. 22:1–11.

Jovanovic K, Vranic J, Miljkovic N. 2015. Hill's and Huxley's muscle models - tools for simulations in biomechanics. Serb J Electr Eng. 12(1):53–67.
Kaplan ML, Heegaard JH. 2001. Predictive algorithms for neuromuscular control of human locomotion. J Biomech. 34(8):1077.
Klein T, Lewis MA. 2012. A neurorobotic model of bipedal locomotion based on principles of human neuromuscular architecture. Proceedings of the IEEE International Conference on Robotics and Automation, St. Paul, MN, USA.
McLean SG, Su A, van den Bogert AJ. 2003. Development and validation of a 3-D model to predict knee joint loading during dynamic movement. J Biomech Eng. 125(6):864–874.
Pandy MG, Berme N. 1988. A numerical method for simulating the dynamics of human walking. J Biomech. 21(12):1043–1051.
Park J. 2008. Synthesis of natural arm swing motion in human bipedal walking. J Biomech. 41(7):1417–1426.
Pizzolato C, Reggiani M, Modenese L, Lloyd D. 2017. Real-time inverse kinematics and inverse dynamics for lower limb applications using OpenSim. Comput Methods Biomech Biomed Eng. 20(4):436–445.
Rajagopal A, Dembia CL, Demers MS, Delp DD, Hicks JL, Delp SL. 2016. Full body musculoskeletal model for muscle-driven simulation of human gait. IEEE Trans Biomed Eng. 63(10):2068–2079.
Seok S, Wang A, Otten D, Kim S. 2012. Actuator design for high force proprioceptive control in fast legged locomotion. Proceedings of the IEEE/RSJ International Conference on Intelligent Robots and Systems, Vilamoura-Algarve, Portugal.
Seth A, Sherman M, Reinbolt JA, Delp SL. 2011. OpenSim: a musculoskeletal modeling and simulation framework for in silico investigations and exchange. Procedia IUTAM. 2:212–232.
Thelen DG, Anderson FC. 2006. Using computed muscle control to generate forward dynamic simulations of human walking from experimental data. J Biomech. 39(6):1107–1115.
van den Bogert AJ, Schamhardt HC, Crowe A. 1989. Simulation of quadrupedal locomotion using a rigid body model. J Biomech. 22(1):33.
van Soest AJ, Bobbert MF. 1993. The contribution of muscle properties in the control of explosive movements. Biol Cybern. 69(3):195–204.

Appendix

The purpose of kinematics modeling of human lower limbs is to determine the motion relationship among the joints of human lower limbs. Its essence is to solve the angle, angular velocity, and angular acceleration of swinging limbs and to express the relative position and motion relationship between the joints. For the human lower limb model, the generalized coordinate system of the human lower limb system is established first, and then the state of the lower limb system is represented by nine coordinates. The generalized coordinate system is shown in Figure A1.

In the figure, X and Y, respectively, represent the transverse and vertical coordinates of the upper ends of the torso in the world coordinate system; $q_1 \dots q_7$ are the angles between each limb part and the Y direction of the world coordinate system (assuming that the anticlockwise direction is positive); $m_1 \dots m_7$ are the masses of the trunk, thighs, calves, and feet ($m_2{=}m_3$, $m_4{=}m_5$, $m_6{=}m_7$); $l_1 \dots l_7$ are the vertical distances from the trunk, thighs, calves, and ankle joints to the mass center of the foot, respectively ($l_2{=}l_3$, $l_4{=}l_5$, $l_6{=}l_7$); $A1 \dots A5$ represent each joint; and $C1 \dots C7$ represent each body centroid. Assuming that the center of mass of the system is at the geometric center of the rod, the centroid of the foot is at the location of $l6$ and $l7$ of the ankle from the vertical line between the ankle and the plantar.

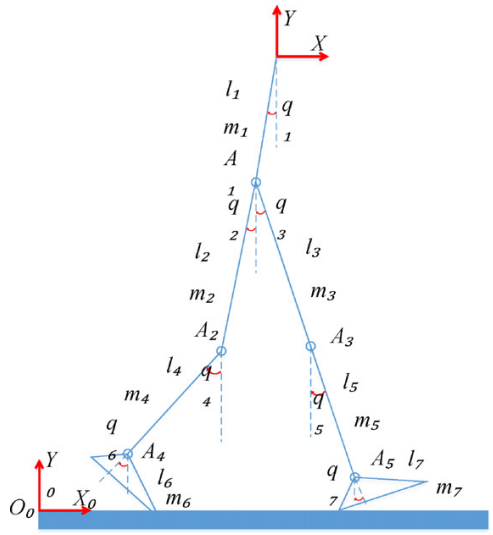

Figure A1. Generalized coordinate system of the lower limb model.

According to the above system model, the position relationship of each joint and centroid of the limb is established as follows (taking one leg as an example, the other relevant formulas can be deduced by using the same equations):

$$X_{A_1} = X - l_1 \sin q_1;\ Y_{A_1} = Y - l_1 \cos q_1. \tag{A-1a}$$

$$\begin{aligned} X_{A_2} &= X - l_1 \sin q_1 - l_2 \sin q_2 \\ Y_{A_2} &= Y - l_1 \cos q_1 - l_2 \cos q_2 \end{aligned} \tag{A-1b}$$

$$\begin{aligned} X_{A_4} &= X - l_1 \sin q_1 - l_2 \sin q_2 - l_4 \sin q_4 \\ Y_{A_2} &= Y - l_1 \cos q_1 - l_2 \cos q_2 - l_4 \cos q_4 \end{aligned} \tag{A-1c}$$

$$X_{C_1} = X - \frac{1}{2} l_1 \sin q_1;\ Y_{C_1} = Y - \frac{1}{2} l_1 \cos q_1. \tag{A-2a}$$

$$\begin{aligned} X_{C_2} &= X - l_1 \sin q_1 - \frac{1}{2} l_2 \sin q_2 \\ Y_{C_2} &= Y - l_1 \cos q_1 - \frac{1}{2} l_2 \cos q_2 \end{aligned} \tag{A-2b}$$

$$\begin{aligned} X_{C_4} &= X - l_1 \sin q_1 - l_2 \sin q_2 - \frac{1}{2} l_4 \sin q_4 \\ Y_{C4} &= Y - l_1 \cos q_1 - l_2 \cos q_2 - \frac{1}{2} l_4 \cos q_4 \end{aligned} \tag{A-2c}$$

$$\begin{aligned} X_{C_6} &= X - l_1 \sin q_1 - l_2 \sin q_2 - l_4 \sin q_4 - l_6 \sin q_6 \\ Y_{C6} &= Y - l_1 \cos q_1 - l_2 \cos q_2 - l_4 \cos q_4 - l_6 \cos q_6 \end{aligned} \tag{A-2d}$$

The absolute velocity relationship of the body centroid position can be written as follows:

$$\begin{aligned}\dot{X}_{C_1} &= \dot{X} - \frac{1}{2} l_1 \dot{q}_1 \cos q_1 \\ \dot{Y}_{C_1} &= \dot{Y} + \frac{1}{2} l_1 \dot{q}_1 \sin q_1 \\ \dot{\varphi}_{C_1} &= \dot{q}_1\end{aligned} \tag{A-3a}$$

$$\begin{aligned}\dot{X}_{C_2} &= \dot{X} - l_1 \dot{q}_1 \cos q_1 - \frac{1}{2} l_2 \dot{q}_2 \cos q_2 \\ \dot{Y}_{C_2} &= \dot{Y} + l_1 \dot{q}_1 \sin q_1 + \frac{1}{2} l_2 \dot{q}_2 \sin q_2 \\ \dot{\varphi}_{C_2} &= \dot{q}_1 + \dot{q}_2\end{aligned} \tag{A-3b}$$

$$\begin{aligned}\dot{X}_{C_4} &= \dot{X} - l_1 \dot{q}_1 \cos q_1 - l_2 \dot{q}_2 \cos q_2 - \frac{1}{2} l_4 \dot{q}_4 \cos q_4 \\ \dot{Y}_{C_4} &= \dot{Y} + l_1 \dot{q}_1 \sin q_1 + l_2 \dot{q}_2 \sin q_2 + \frac{1}{2} l_4 \dot{q}_4 \sin q_4 \\ \dot{\varphi}_{C_4} &= \dot{q}_1 + \dot{q}_2 + \dot{q}_4\end{aligned} \tag{A-3c}$$

$$\begin{aligned}\dot{X}_{C_6} &= \dot{X} - l_1 \dot{q}_1 \cos q_1 - l_2 \dot{q}_2 \cos q_2 - l_4 \dot{q}_4 \cos q_4 - l_6 \dot{q}_6 \cos q_6 \\ \dot{Y}_{C_6} &= \dot{Y} + l_1 \dot{q}_1 \sin q_1 + l_2 \dot{q}_2 \sin q_2 + l_4 \dot{q}_4 \sin q_4 + l_6 \dot{q}_6 \sin q_6 \\ \dot{\varphi}_{C_6} &= \dot{q}_1 + \dot{q}_2 + \dot{q}_4 + \dot{q}_6\end{aligned} \tag{A-3d}$$